Available online at www.sciencedirect.com
SCIENCE DIRECT®
Carbohydrate Research 340 (2005) 929–941
Carbohydrate RESEARCH

Hyaluronan conformations on surfaces: effect of surface charge and hydrophobicity

Chiara Spagnoli,[a] Alexander Korniakov,[a] Abraham Ulman,[a] Endre A. Balazs,[b] Yuri L. Lyubchenko[c] and Mary K. Cowman[a,*]

[a]*Othmer Department of Chemical and Biological Sciences and Engineering, Polytechnic University, 6 Metrotech Center, Brooklyn, NY 11201, USA*
[b]*Matrix Biology Institute, 65 Railroad Avenue, Ridgefield, NJ 07657, USA*
[c]*Department of Pharmaceutical Sciences, University of Nebraska Medical Center, 986025 Nebraska Medical Center, Omaha, NE 68198-6025, USA*

Received 13 September 2004; accepted 20 January 2005

Dedicated to Professor David A. Brant, in honor of his pioneering work on carbohydrate conformation

Abstract—Extended, relaxed, condensed, and interacting forms of the polysaccharide hyaluronan have been observed by atomic force microscopy (AFM). The types of images obtained depend on the properties of the surfaces used. We have investigated several different surface conditions for HA imaging, including unmodified mica, mica chemically modified with two different kinds of amino-terminated silanes (3-aminopropyltriethoxysilane and *N*-trimethoxysilylpropyl-*N*,*N*,*N*-trimethylammonium chloride), and highly oriented pyrolytic graphite. We found the degree of HA molecular extension or condensation to be variable, and the number of bound chains per unit area was low, for all of the mica-based surfaces. HA was more easily imaged on graphite, a hydrophobic surface. Chains were frequently observed in high degrees of extension, maintained by favorable interaction with the surface after molecular combing. This observation suggests that the HA macromolecule interacts with graphite through hydrophobic patches along its surface. AFM studies of HA behavior on differing surfaces under well-controlled environmental conditions provides useful insight into the variety of conformations and interactions likely to be found under differing physiological conditions.

Keywords: Hyaluran; Polysaccharide; Atomic force microscopy; Graphite; Conformation; Surface

1. Introduction

Atomic force microscopy (AFM) is an instrumental technique used for imaging of biological molecules deposited on surfaces. Successful AFM imaging requires the interaction between the substrate and the deposited material to be strong enough to avoid displacement of the sample by the AFM probe tip. As a result, immobilization techniques, which can affect the molecular conformations of the deposited material, are often employed in imaging experiments. Therefore, it is necessary to carefully evaluate whether the images obtained are representative of the conformations of a biological sample under physiological conditions, or are a consequence of the interaction of the material with the substrate. If sample–substrate interactions play a significant role, then manipulation of those interactions can provide a different type of insight into the conformational properties of the sample. For example, if a molecule has more than one physiolo-gically relevant conformation, triggered by changes in solvent environment, presence of interacting molecular species, etc., then one may also see the evidence for that conformational versatility in AFM images obtained under varying conditions.

Hyaluronan (HA) is a negatively charged polysaccharide found in extracellular, cell surface, and intracellular environments. It exhibits hydrodynamic behavior

* Corresponding author. Tel.: +1 718 260 3054; fax: +1 718 260 3125; e-mail: mcowman@poly.edu

0008-6215/$ - see front matter © 2005 Elsevier Ltd. All rights reserved.
doi:10.1016/j.carres.2005.01.024

typical of a slightly stiffened random coil in dilute aqueous salt solution.[1–8] AFM imaging of HA on mica surfaces has shown a variety of chain conformations and intramolecular and intermolecular interactions, but the most notable property of HA on mica is a rather strong tendency to form aggregates, even when deposited at low concentrations.[9–17] Although the aggregate formation has been attributed to an intrinsic tendency for HA to form networks,[9,12] the evidence for such networks in solution remains elusive.[8,18–23] An alternative explanation for the network formation may be considered to derive from sample–surface interactions. The relevant surface properties include the nature of the mica surface itself, as well as the thickness of the hydration layer, the extent of structuring of the water, the effective dielectric constant, the effective ionic strength, and correlation effects in ionic distributions.[24] The microenvironment at the surface could favor HA self-association over HA–mica interactions. A more complete understanding of the dependence of HA conformation and interactions on local surface characteristics would be valuable in interpreting the relevance of the AFM observations to the physiological forms and properties of HA, especially when in unique environments such as may be found at the cell surface.

The question of the influence of surface immobilization on the conformation and interactions of biological macromolecules has been most extensively examined for DNA and polysaccharides. In a common sample preparation technique, DNA is immobilized on mica by deposition from solutions containing divalent cations of various metals, such as nickel, cobalt, zinc, manganese, or magnesium.[25,26] These metal cations exchange with potassium ions on the mica surface to form bridges between the negative charges on the surface and on DNA.[27] Polysaccharides have also been deposited on mica using divalent counterions, or alternatively using simple aqueous solutions, sometimes containing a volatile buffer such as ammonium acetate.[28] It has been observed that the details of the deposition and immobilization procedure can affect the apparent degree of extension and conformation of the polymer. The contour length, molecular weight, molecular weight distribution, and apparent persistence length of a polymer can be determined by electron microscopy (EM) or AFM, if the polymer is fully in contact with the surface.[28–32] The degree to which the persistence length on a surface reflects the solution properties of the polymer depend on the strength of the polymer–surface interaction. Two different scenarios are generally considered: the polymer molecules can be kinetically trapped, or be in equilibrium with the surface. If kinetically trapped, the chains resemble two-dimensional projections of the conformations they assumed in solution, with only slight deformations. If at equilibrium, the molecules appear as if they are in a two-dimensional solution. Under the equilibrated condition, the persistence length calculated from AFM images can match that of a polymer in solution, after taking the difference in dimensionality into account. It is important to note that the proper conditions for equilibration are not generally known in advance, but require matching of the images with the known persistence length. Potential sources of error in determining the persistence length include incomplete attachment and flattening of the polymer on the surface, orientation and extension of polymer molecules caused by sample deposition and drying procedures, and strong adhesion of the chains to the surface at a limited number of points, thus constraining the molecular relaxation on the surface.[28,30–36]

Alternative surfaces that may provide better attachment and equilibration of biological macromolecules than bare mica have been investigated. One such substrate, used successfully for attachment of DNA, is 3-aminopropyltriethoxysilane (APTES) modified mica (AP-mica),[37] a surface functionalized with amino groups. XPS measurements[38] on an AP-mica showed that the fraction of amino groups pointing toward the surface was no more than 10% of the total number. About 50% of these amines were protonated, and therefore capable of interacting electrostatically with DNA. Thus the surface has a low density of positive charges. The binding of DNA to AP-mica affords a stronger interaction than that to bare mica. Supercoiled and bent DNA have been observed to retain conformations similar to those assumed in solution when deposited on such substrates.[39–45]

The influences of surfaces on the form of ordered condensates and assemblies of macromolecules have also been observed by AFM. For example, DNA and polysaccharide condensates have been deposited on bare mica and imaged in air[46,47] and in liquid.[48] Mica surfaces treated with APTES, spermine or spermidine have also been used for DNA condensate imaging in air,[49,50] and it was found that the structure of supercoiled DNA in solution was close to that observed on mica treated with spermine. Incomplete condensates have been imaged in air using poly-L-ornithine-coated mica, a substrate that showed higher affinity for DNA and allowed kinetic trapping of forming toroids.[51] Interestingly, surface-directed condensation in the absence of multivalent cations has also been observed.[52] Differences between DNA condensation on mica and in solution have also been observed: in the presence of protamine, toroids appeared to be larger when condensation took place on the surface.[53] There is also evidence that the morphology of the condensed forms observed by AFM can be dependent on sample preparation and drying methods used for imaging in air.[46,53]

Knowledge of the effects of surface conditions on DNA conformation and condensation can be applied to the study of molecules like HA, after due consider-

ation of the differences in structure. Both molecules are negatively charged polyelectrolytes. DNA is much more rigid than HA, due to its double helical conformation. The persistence length for DNA chains in solution is in the range of 50 nm,[29] while for HA it is about 10 times smaller.[3,5,6] Secondly, the strong affinity of DNA for mica in the presence of divalent cations[26,27] is very different from the tendency to self-aggregate observed by AFM for HA[9–17] when deposited on the same substrate. DNA is also a much thicker molecule, ca. 2 nm versus 0.5 nm for HA. This may be a very important consideration, as the molecular dimension relative to the thickness of the surface hydration layer may determine effective hydration of the macromolecule. It therefore seems necessary to independently establish the dependence of HA conformation and equilibration on differing surface properties.

Biological molecules often perform their functions while in close proximity to surfaces. Thus their interactions with artificial substrates can give insight into the effects of various surface types on macromolecular conformation and interactions. This is an important consideration for HA, which can be found in contact with the cell surface and the extracellular matrix, as well as intracellular locations. The purpose of this study is to evaluate the effect of surface chemistry on possible conformations of HA, with particular attention to the occurrence of condensates. This is a step toward understanding of the relationship between the conformational transitions and the biological functions of the polysaccharide.

2. Results

2.1. Surface modification and characterization

The mica surface was modified by silylating agents (Fig. 1) through the reaction of surface hydroxyl groups. The general scheme[37,49] for this reaction is

$$SiOH + X_3SiY \rightarrow SiO - SiX_2\text{-}Y$$

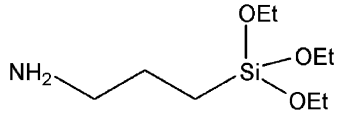

3-Aminopropyltriethoxysilane

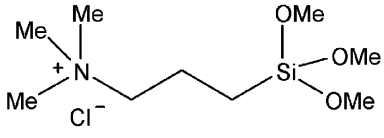

N-trimethoxysilylpropyl-*N*,*N*,*N*-trimethylammonium chloride

Figure 1. Structures of the silane derivatives used to modify mica.

where SiOH groups belong to the mica surface, X is a hydrolyzable group, such as (CH_3CH_2O–) for APTES, responsible for the covalent bonding of the modifying reagent with the surface, and Y is chosen based on its ability to interact with the sample. In this study, Y stands for $(CH_2)_3NH_2$ and $(CH_2)_3NH_3^+$ for AP-mica, and $(CH_2)_3N(CH_3)_3^+$ for TMSPTA-modified mica. Because these modifications leave cationic amino groups exposed and capable of interacting with the sample, such surfaces have been extensively used to image DNA under a variety of conditions.

To verify the modification of the surface properties, root-mean-square (RMS) roughness measurements, as well as contact angle measurements for the surfaces, were performed. Table 1 shows the results of these measurements. By performing the surface modification in a vapor phase of the corresponding modifying reagent, it was possible to achieve a surface roughness low enough ($\leqslant$0.3 nm) to allow imaging of thin (ca. 0.5 nm) HA chains. The static contact angle we observed (this study and previous study[54]) for a pre-hydrated mica surface ($23 \pm 1°$) was higher than the previously reported value of $8.0 \pm 1°$ measured for freshly cleaved mica substrates.[55] We were unable to measure the contact angle of freshly cleaved mica, since the droplet spreads rapidly and completely wets the surface, possibly due to electrostatic effects.

Contact angles on amino-modified surfaces were observed to be similar to each other, and in all instances the surfaces showed lower wetting in comparison with unmodified prehydrated mica. The modified surfaces thus presented relatively higher degrees of hydrophobicity in comparison with the untreated mica.[56] This could be attributed to the presence of the short aliphatic fragment in the chemical structure of each modifying agent (Fig. 1), which affects the affinity of the surface toward water, even in the presence of positive charges, as in the case of TMSPTA. The value of the water contact angle obtained for the AP-mica ($31 \pm 1°$) is much lower in comparison with the previously reported[57] advancing (63°) and receding (59°) values measured for APTES-modified silica. However, these results are consistent with the surface preparation methods: previously, modified silica surfaces were prepared by drop deposition of the modifying agent, while in this study, the surface modification of the mica was carried out by vapor-phase deposition of the

Table 1. Values of roughness and contact angles for the substrates used for AFM imaging of HA

Surface	Contact angle	Roughness (RMS) (nm)
Mica	$23 \pm 1°$	0.083
APTES mica	$31 \pm 1°$	0.271
TMSPTA mica	$36 \pm 1°$	0.258
Graphite	$79 \pm 1°$	0.133

surface-modifying reagent.[37] By using this technique, less rough surfaces were produced. The modified mica surfaces were not atomically flat; they displayed higher roughness in comparison with the untreated mica, as expected since the presence of clusters of the modifying reagent was observed previously.[56] At the same time, these chemically modified substrates were still suitable for HA imaging since the diameter of the polysaccharide chain was in the range of 0.5 nm.

We also analyzed the surface characteristics of the graphite samples. The contact angle measurements for the graphite surfaces (79 ± 1°) compared favorably with the reported value of 83 ± 1°,[55] confirming its relative hydrophobicity. The higher value of the roughness obtained for graphite surfaces as compared to untreated mica was attributed to the frequent occurrence within a small surface area of multiple surface-exposed layers, linked by steps, for graphite. These were produced during the graphite cleavage process, and contributed to the overall value of the surface roughness.

2.2. HA on mica and modified mica

HA shows high conformational variability when deposited on pure mica. In previous studies,[10,11,15–17] we showed that HA chains could appear in varying degrees of extension, ranging from straight, fully extended chains, through partially relaxed and fully relaxed coiled forms, to chains with varying degrees of condensation, including the pearl-necklace and condensed rod forms. (Here, the term 'relaxed coil' means a chain having an apparent degree of coiling consistent with the dilute solution conformation of the chain.) Quantitating the relative frequency of occurrence of the different conformations is complicated because there is not a set of discrete shapes, but rather a continuum of conformations between extended and condensed chains. There are also very few isolated chains bound to mica; on average less than 1 isolated chain per 10 μm^2 is found. On freshly cleaved mica, we found roughly 30% relaxed coil chains and 70% substantially condensed chains for 366 isolated chains imaged. On mica prehydrated by exposure to ambient humidity, we found roughly 80% extended chains and 20% substantially condensed chains for 156 isolated chains imaged. In the present work, we provide selected images of HA on unmodified mica solely as representative control data for the particular HA samples to be used elsewhere in this study on the effect of differing surfaces. Moderate molecular weight HA, deposited on freshly cleaved or prehydrated mica from a 10 μg/mL aqueous solution, was observed to adopt structures ranging from relaxed coil conformations (Fig. 2A, on

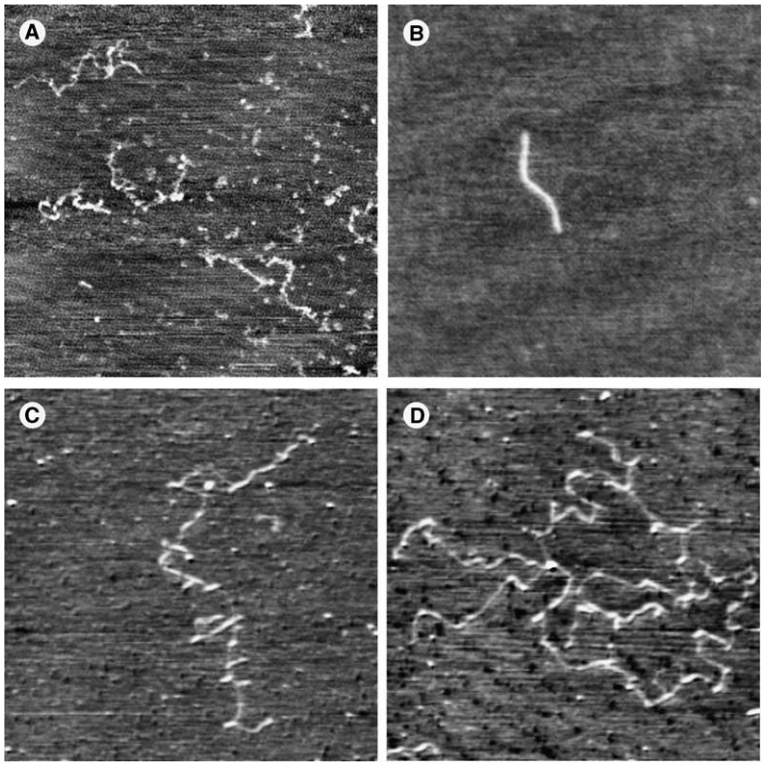

Figure 2. TMAFM height images of HA chains deposited on unmodified mica. (A) Moderate MW HA deposited from 10 μg/mL solution in H_2O. Image size 1 μm × 1 μm × 0.9 nm. (B) Moderate MW HA deposited from 10 μg/mL solution in H_2O. Image size 750 nm × 750 nm × 1.3 nm. (C) High MW HA deposited from 10 μg/mL solution in H_2O. Image size 1.25 μm × 1.25 μm × 2.3 nm. (D) High MW HA deposited from 10 μg/mL solution in H_2O. Image size 1.3 μm × 1.3 μm × 2.5 nm.

freshly cleaved mica) to fully condensed ones in the form of compact, thick rods (Fig. 2B, on prehydrated mica). Under the same conditions, the high molecular weight HA sample typically assumed partially extended, partially condensed conformations on prehydrated mica, identified by the occurrence of brighter, rigid segments along the chain linked by the more relaxed portions of the chains, as illustrated in Figure 2C and D.

HA deposited onto AP-mica showed a similar variety of conformations. For 65 chains imaged, we found roughly 20% of chains in extended shapes and 80% in partially or fully condensed forms. Moderate molecular weight HA typically showed extended or partially condensed conformations (Fig. 3A and B). High molecular weight HA samples also showed variable degrees of condensation ranging from extended to almost fully condensed, including some particularly good examples of the pearl-necklace conformations, as illustrated in Figure 3C and D.

Mica modified with the quaternary alkylamine TMSPTA also allowed HA to adopt a variety of structures differing in degree of condensation. Moderate molecular weight HA could appear as loosely coiled chains or more rigid (extended or possibly partially condensed) conformations (Fig. 4A and B). The same was true for high molecular weight HA (Fig. 4C and D). It was not always possible to determine if the rigid chains were extended or condensed, since the chain heights, especially measured against a rougher surface, can be insufficiently accurate for that use. The number of useable images obtained for HA on the TMSPTA modified surfaces was also small, reflecting the generally weak affinity of HA for the surface, and the inherent roughness of the surface. For 46 isolated chains imaged, roughly 20% were extended, 20% relaxed coil, and 60% substantially or completely condensed.

In general, imaging of HA on modified mica surfaces presented the same difficulties encountered when imaging on unmodified mica, and there seemed to be no advantage in the use of such surfaces for HA, in terms of higher occurrence of extended, relaxed, or condensed conformations. Furthermore, larger globules deriving from aggregation of numerous molecules were often observed; these were similar to those imaged on mica. The number of chains found was also similar, indicating no significant increase in affinity of HA for the chemically modified, positively charged, surfaces.

2.3. HA on graphite

Dramatic differences were seen when HA was deposited on graphite. Moderate molecular weight HA deposited

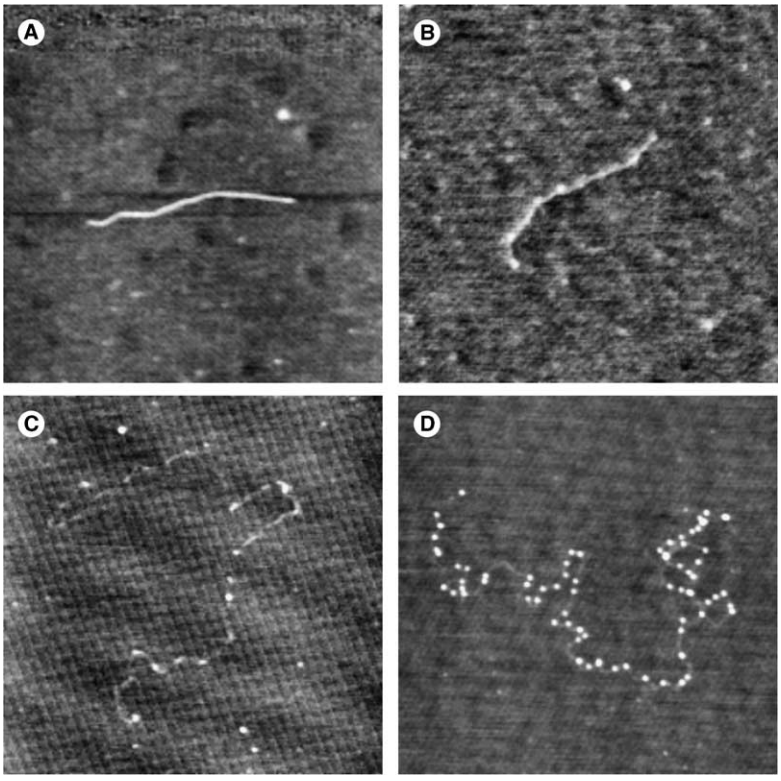

Figure 3. TMAFM height images of HA chains deposited on APTES-modified mica. (A) Moderate MW HA deposited from 10 μg/mL solution in H_2O. Image size 1 μm × 1 μm × 1.5 nm. (B) Moderate MW HA deposited from 10 μg/mL solution in H_2O. Image size 750 nm × 750 nm × 0.9 nm. (C) High MW HA deposited from 10 μg/mL solution in H_2O. Image size 1.5 μm × 1.5 μm × 0.7 nm. (D) High MW HA deposited from 10 μg/mL solution in 3 mM NaCl. Image size 1.5 μm × 1.5 μm × 2 nm.

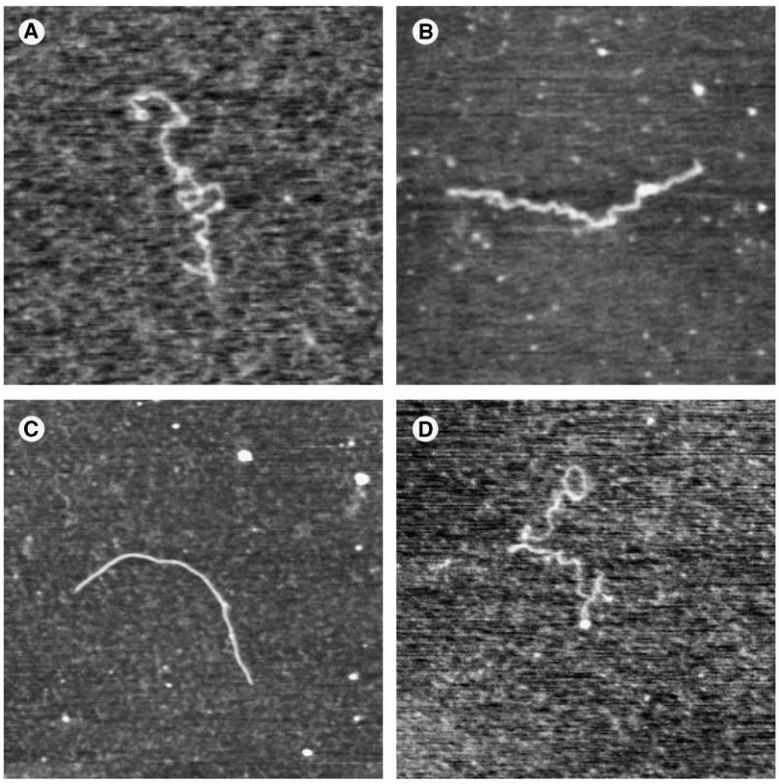

Figure 4. TMAFM height images of HA chains deposited on TMSPTA-modified mica. (A) Moderate MW HA deposited from 10 μg/mL solution in H_2O. Image size 750 nm × 750 nm × 1.3 nm. (B) Moderate MW HA deposited from 10 μg/mL solution in H_2O. Image size 750 nm × 750 nm × 1.7 nm. (C) High MW HA deposited from 10 μg/mL solution in H_2O. Image size 1.25 μm × 1.25 μm × 3 nm. (D) High MW HA deposited from 10 μg/mL solution in H_2O. Image size 1 μm × 1 μm × 1 nm.

from a relatively concentrated solution (100 μg/mL) showed a large number of chains bound to the graphite surface, but contracted into globular forms (Fig. 5A). That image is noteworthy because it shows that the chains were not entangled with each other either in solution or on the surface, but remained well separated. On mica, the chains would usually show significant intermolecular aggregation under the same circumstances. Figure 5B and C shows moderate molecular weight HA deposited on graphite at the usual low concentration of 10 μg/mL. Both globular condensed forms and isolated chains clearly showing extension under the influence of molecular combing can be observed. Images of the high molecular weight HA samples deposited on graphite showed long, combed aggregates of molecules interacting side by side (Fig. 5D–F). Here, the tendency of the chains to interact with each other was readily observed, but the high degree of extension clearly indicated the establishment of favorable interactions with the surface. In all of the images of HA deposited on graphite from 10 μg/mL solution, the number of chains was surprisingly high (usually greater than 10 chains per 10 μm^2) in comparison with the results for mica and modified mica, which shows that HA binds more strongly to the graphite surface.

2.4. Comparison of HA deposited on differing surfaces without rinsing

Both the moderate and high molecular weight HA seemed to establish more favorable interactions with the graphite surface than with the freshly cleaved or chemically modified mica. To further confirm this observation, samples were prepared on mica and graphite, omitting the rinsing step. Thus, the surfaces were dried with a gentle flow of nitrogen after the sample deposition and a defined incubation period. The different behavior of the polysaccharide left to dry on mica versus graphite was obvious (compare Figs. 6 and 7). Moderate molecular weight HA chains deposited on graphite usually appeared to be partially extended by molecular combing (Fig. 6A–C). Some intermolecular association was also observed, arising probably from the drying step, but these chains appeared to be mostly separated. Many chains, incompletely combed, were observed on graphite in the case of high molecular weight hyaluronan (Fig. 6D–F). Side-by-side interchain interactions, forming web-like aggregates, could be observed. In other cases, chains formed apparently helical coils (Fig. 6E).

When the rinsing step was omitted for HA deposited on a hydrophilic bare mica surface, there was a high

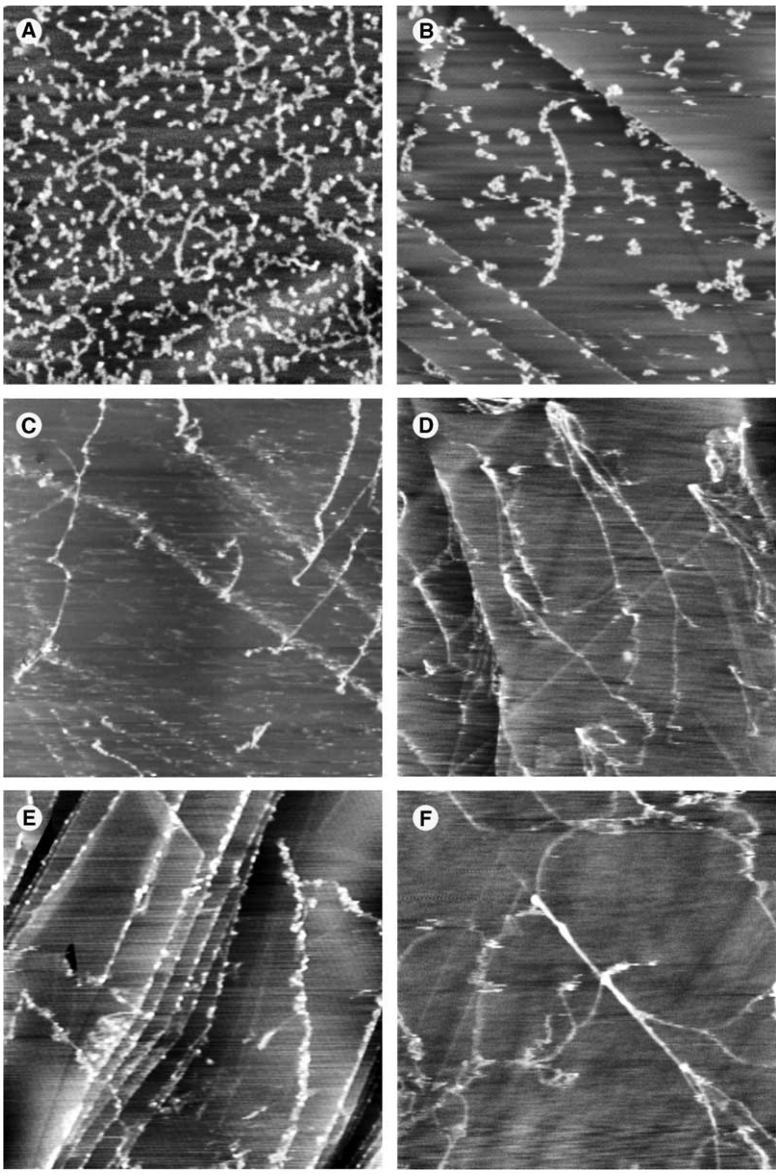

Figure 5. TMAFM height images of HA chains deposited on graphite. (A) Moderate MW HA deposited from 100 μg/mL solution in H_2O. Image size 1.5 μm × 1.5 μm × 2.2 nm. (B) Moderate MW HA deposited from 10 μg/mL solution in H_2O. Image size 1 μm × 1 μm × 4.5 nm. (C) Moderate MW HA deposited from 10 μg/mL solution in H_2O. Image size 2.75 μm × 2.75 μm × 4 nm (D) High MW HA deposited from 10 μg/mL solution in 3 mM NaCl. Image size 3 μm × 3 μm × 2 nm. (E) High MW HA deposited from 10 μg/mL solution in H_2O. Image size 3 μm × 3 μm × 2.7 nm. (F) High MW HA deposited from 10 μg/mL solution in 3 mM NaCl. Image size 1.5 μm × 1.5 μm × 1.3 nm.

number of chains present. The appearance of moderate molecular weight HA chains was not much affected (Fig. 7A and B), but for high molecular weight HA large interacting networks of chains were observed (Fig. 7C and D). The linkage points in the networks were globular aggregates formed as a result of the drying process and the low affinity of the polysaccharide for the surface. Fibers composed of two or more chains interacting with each other extended between the formed globules. Their occurrence derived from the fact that those chains were shared between the aggregates; hence, they were forced to assume elongated conformations on the surface. The molecules forming those fibers appeared to be interacting with each other in twisted helical ropes (Fig. 7D).

3. Discussion

3.1. HA on mica and charge-modified mica surfaces

The occurrence of extended, relaxed, condensed, and interacting forms of HA on unmodified mica has been previously observed.[9–17] The tendency to adopt one type of conformation has been correlated with the hydration state of the mica surface at the time of sample

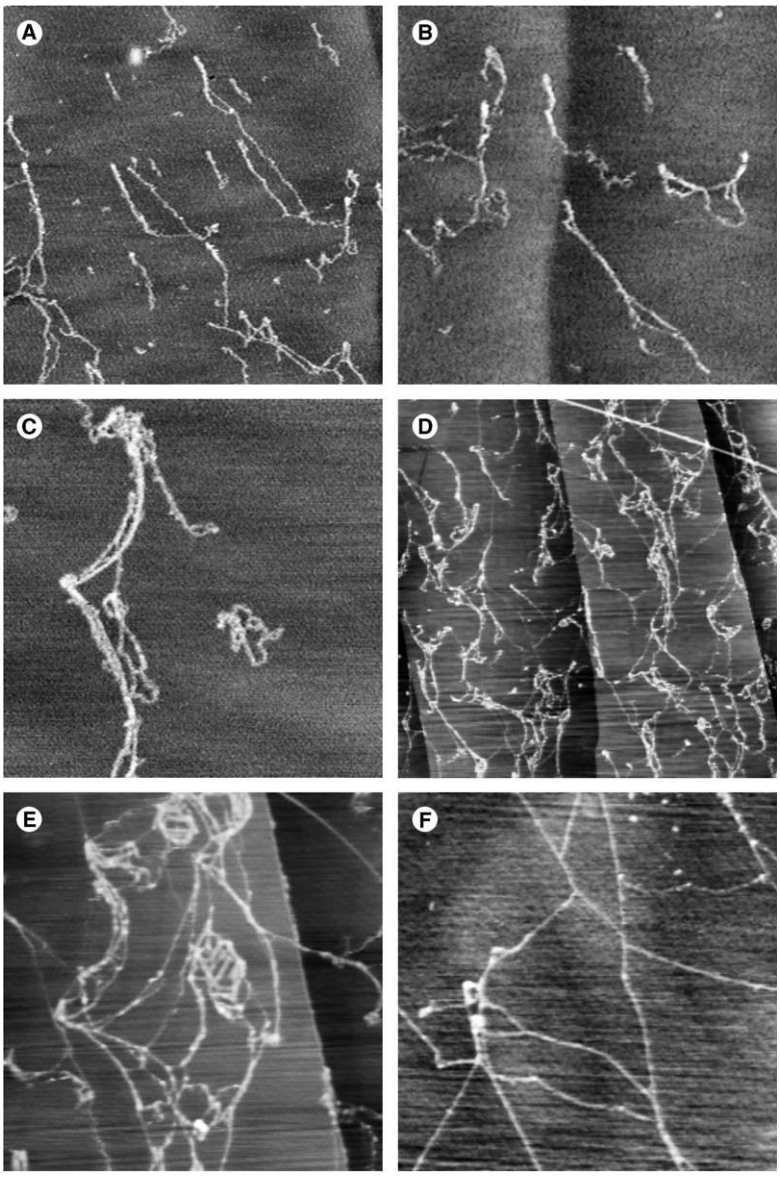

Figure 6. TMAFM height images of HA chains deposited on graphite and not rinsed before drying. (A) Moderate MW HA deposited from 10 μg/mL solution in H_2O. Image size 3 μm × 3 μm × 1.9 nm. (B) Moderate MW HA deposited from 10 μg/mL solution in H_2O. Image size 1.5 μm × 1.5 μm × 1.8 nm. (C) Moderate MW HA deposited from 10 μg/mL solution in H_2O. Image size 900 nm × 900 nm × 2 nm. (D) High MW HA deposited from 10 μg/mL solution in H_2O. Image size 3 μm × 3 μm × 4 nm. (E) High MW HA deposited from 10 μg/mL solution in H_2O. Image size 1 μm × 1 μm × 6 nm. (F) High MW HA deposited from 10 μg/mL solution in H_2O. Image size 1.5 μm × 1.5 μm × 1.6 nm.

deposition.[16,17,54] When mica was cleaved and exposed to ambient conditions (room temperature and relative humidity) long enough for a thin layer of structured water to form, the images of deposited HA showed the prevalence of extended conformations, created by the mechanical force of molecular combing by a moving droplet of water across the surface, followed by strong adhesion of the extended chain to the water layer. The HA chains were shown to lie on top of the structured water. On freshly cleaved mica, the occurrence of extended forms was lower, and imaging was generally much more difficult. The HA chains were submerged in the forming structured water layer, acted as defects in the water structure, and adopted relaxed forms similar to the solution conformation of HA. More condensed structures could also form, under conditions appropriate for counterion-mediated polyelectrolyte attraction.[17,58–61] These relaxed and condensed structures appear to arise when HA molecules recoil after combing and/or self-condense due to weak attachment to the mica surface. The inability of mica to bind HA in a low ionic strength solution has recently been studied in detail by Tadmor et al.[62] Hence, the polysaccharide showed stronger affinity for the structured water surface

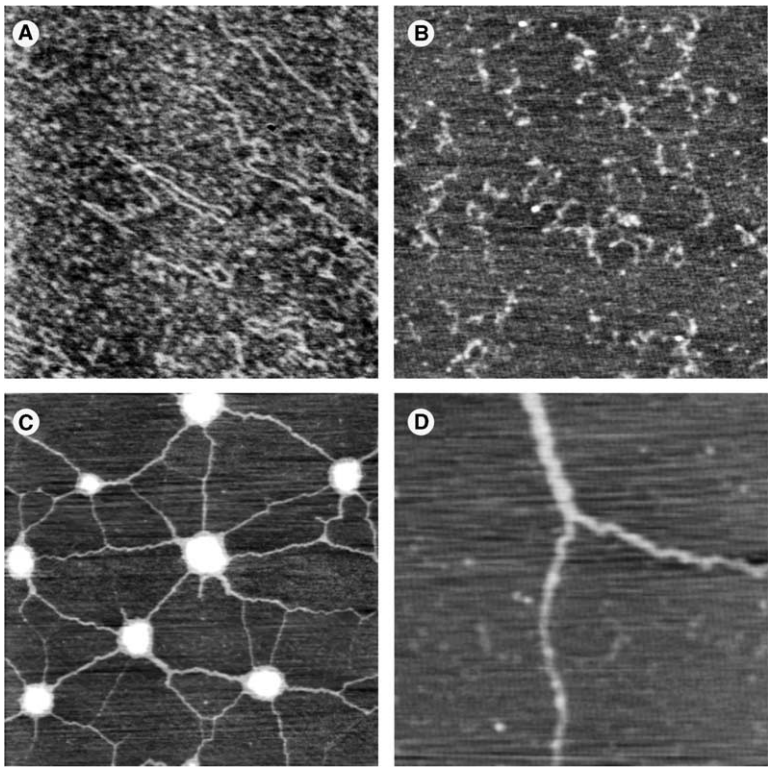

Figure 7. TMAFM height images of HA chains deposited on unmodified mica and not rinsed before drying. (A) Moderate MW HA deposited from 10 μg/mL solution in H_2O. Image size 3 μm × 3 μm × 0.8 nm. (B) Moderate MW HA deposited from 10 μg/mL solution in H_2O. Image size 1 μm × 1 μm × 1.2 nm. (C) High MW HA deposited from 10 μg/mL solution in H_2O. Image size 3 μm × 3 μm × 3 nm. (D) High MW HA deposited from 10 μg/mL solution in H_2O. Image size 750 nm × 750 nm × 2.7 nm.

than for the mica surface itself, probably as a consequence of the establishment of hydrogen bonds with the underlying structured water layer.

One goal of the present work was to determine whether a charge-modified mica surface could bind HA more strongly. Chemical modification of mica with 3-aminopropyltrimethoxysilane (APTES) or *N*-trimethoxysilylpropyl-*N*,*N*,*N*-trimethylammonium chloride (TMSPTA) resulted in pendant cationic groups at the ends of short aliphatic chains covalently bound to the mica surface. In the case of APTES derivatization, the surface obtains only a low charge density.[38,56] As a result, macromolecules like DNA can often be immobilized without drastic modification of the conformations assumed in solution.[39] Derivatization of mica with the fully charged TMSPTA also produces a positively charged surface, but the charge density has not been measured.

A thin film of water exists on mica surfaces at ambient temperature and humidity, and is at least partially structured.[54,63–72] On unmodified mica, the hexagonal unit cell of the structured water is believed to lie in epitaxial relation with the underlying hexagonal unit cell of the surface, as suggested by the similarity of the dimensions of the two unit cells (0.48 nm for ice 1 h vs 0.51 nm for mica). Modification of the mica by derivatization with pendant groups can constitute an obstacle for the structuring of the water layer on the mica. It is likely that the water layer on the modified mica surfaces is less structured than on bare mica.

The affinity of HA for the functionalized micas was not observed to be significantly greater than that seen for unmodified mica, based on the average number of chains immobilized and imaged. Similarly, the conformational behavior of the polysaccharide on modified mica was not significantly different from that observed when it was imaged on unmodified mica. The same range of extended, relaxed, and condensed conformations were observed for HA on modified and unmodified mica. It is possible, however, that there is some weak attractive electrostatic interaction between HA and the cationic groups on the modified mica. The observation of some extended HA chains, if not stabilized by structured water in the case of modified mica, could be attributed to inhibition of chain recoil by the interaction with the cationic groups. It is also of interest that the nearly perfect pearl necklace structure observed on AP-mica (Fig. 3D) could have arisen through specific attachments of the HA chain to cationic groups on the surface, followed by condensation of intervening chain segments. With that said, we note that self-assembled monolayers of short-chain adsorbates are highly disordered,

especially with polar surface groups such as OH or NH_2. This results from the tendency of a high-energy surface exposed to a low dielectric medium (air) to reduce the surface energy through *trans–gauche* conformational changes. This results in the exposure of the terminal methylene groups, thus reducing surface energy. Therefore, studies are planned where surfaces are modified with rigid surfactants carrying ammonium groups at their termini. This will eliminate conformational freedom, thus providing controlled molecularly engineered surfaces for AFM studies.

3.2. HA on graphite surfaces

The presence of water on graphite has been studied by various methods: high-resolution electron energy loss spectroscopy, electronic structure total energy computation, and scanning tunneling microscopy.[73–76] Although a water layer was found to be present on the surface, its topographic imaging was not possible, suggesting that this layer lacked any structure and orientation. The energy of the water molecules located in very close proximity to the surface has previously been calculated to be high, hence it was suggested that the water layer lies at least 0.35 nm above the graphite surface.[55] Graphite surfaces did not seem to influence the structure of the water clusters, suggesting that such clusters form at the points of surface defects, and successively extend.[73]

The behavior of HA deposited on graphite is very different from that of HA on mica. In our studies, we observed the frequent occurrence of extended HA conformations and a higher number of adherent chains on the average graphite sample, suggesting that HA has a quite strong affinity for the graphite surface. Jacoboni et al.[12] previously analyzed HA deposited on graphite and allowed to dry from a 1 mg/mL solution. Their sample showed extensive intermolecular aggregation, and weak attachment to the surface. Our data, obtained for HA samples at lower concentrations, reveal better-separated molecules, with a stronger attachment to the surface. It may be that the HA–HA interactions favored at high concentration can mask the hydrophobic aspects of the HA structure, and limit interaction with the surface. Thus the isolated HA polysaccharide chain, although highly hydrophilic and negatively charged, is capable of interacting favorably with the hydrophobic graphite surface. However, the presence of the structured water layer on the surface cannot, in this case, account for such an observation. As suggested on the basis of molecular modeling studies,[77] the existence of hydrophobic patches along the hyaluronan chain surface could account for the favorable HA–graphite interactions. In general, all polysaccharides having a backbone structure based on glucose residues have hydrophobic groups oriented above and below the average plane of each sugar ring, and hydrophilic groups displayed around the perimeters of the rings. Thus, the combination of hydrophilic and hydrophobic character is an intrinsic part of the backbone structure of HA.

Since graphite is a conductive material, it is also possible to have image charges arise on its surface as a consequence of interactions with a charged species.[78] This could also contribute to the highly favorable HA–graphite interaction, as compared with mica that is an insulating material.

A comparison of the high molecular weight samples represented in Figures 5D–F and 6D–F show that the chains dried on graphite without rinsing established much stronger interactions with the surface than in the case of the well-rinsed samples, which appeared to move under the tip during the scanning. It is possible that the chains, when in contact with excess water during rinsing, tend to mask their hydrophobic patches, and subsequently interact less strongly with the substrate. Movement of the chains during scanning has also been observed in the case of the moderate molecular weight samples, but to a lesser extent. Hence, it could be speculated that the shorter chains were able to adopt more favorable conformations to increase their interactions with the substrates.

The AFM studies of HA samples on graphite have provided unexpected insight into the nature of HA solution properties. Deposition of moderate molecular weight polysaccharide from a relatively concentrated solution (0.1 mg/mL) resulted in the presence of a high number of chains on the substrate. Those molecules were not well extended, but did not show any kind of networking interactions either. This excluded any occurrence of stable associations between the chains in the solution, even at higher concentration, and proved that the networks usually observed on mica surfaces by AFM, especially when the sample was prepared from a diluted solution, are likely to result from the much weaker attraction of HA for mica in comparison with graphite.

4. Conclusions

The behavior of HA on surfaces is the result of interplay between surface–HA and HA–HA interactions. On unmodified mica, HA can adopt extended, relaxed, condensed, and interacting structural motifs. The location of the HA molecule relative to a structured water layer on the mica surface affects the strength of the HA binding to the surface. HA condensation and aggregation on the hydrated mica surface may be driven by counterion-mediated attractive interactions between HA chains having near-complete neutralization of charges in the low dielectric constant environment of the structured water layer.

In an attempt to enhance surface–HA interactions, we investigated HA deposited on mica modified with cationic groups. The charge-modified mica surfaces behaved similarly to unmodified mica, with respect to HA binding.

HA deposited on graphite showed more favorable interaction with the surface. The tendency for HA condensation and self-association was reduced relative to that seen on mica surfaces. The ability of the HA to interact with the hydrophobic graphite surface illustrates the important role the hydrophobic patches on the polysaccharide may play in determining the conformation and binding interactions of HA.

5. Experimental

5.1. Materials

High molecular weight (ca. 4×10^6 g/mol) hyaluronan, sodium salt, (HA) was donated by Matrix Biology Institute, Ridgefield, NJ, while the moderate molecular weight (ca. 4×10^5 g/mol) HA was a kind gift of Genzyme Biosurgery Inc., Cambridge, MA. 3-Aminopropyltriethoxysilane (APTES), *N*,*N*-diisopropylethylamine (Sigma–Aldrich Corp., St. Louis, MO) and *N*-trimethoxysilylpropyl-*N*,*N*,*N*-trimethylammonium chloride (TMSPTA), 50% in MeOH, (Gelest Inc., Morrisville, PA), were used as received. Discs of muscovite mica were obtained from Digital Instruments Inc. (presently, Veeco Instruments Inc.), Woodbury, NY. Highly oriented pyrolytic graphite (HOPG), ZYB grade, was purchased from Advanced Ceramics Corp., Cleveland, OH.

5.2. Surface preparation

Mica used as substrate was either cleaved and prehydrated by incubation overnight at room temperature and ambient relative humidity (usually between 30% and 50%), or used immediately after cleavage. Modified surfaces were prepared in vapors of silylating agents according to previously described procedures.[37] In brief, freshly cleaved mica was placed in a desiccator filled with nitrogen, in the presence of two containers, one filled with 30 μL of the modifying agent (either APTES or TMSPTA), and the other with 10 μL of *N*,*N*-diisopropylethylamine. After 2 h, the cup containing the modifying agent was removed and the desiccator was again purged with nitrogen. The modified surfaces were stored under nitrogen in a desiccator, in the presence of *N*,*N*-diisopropylethylamine, for at least 24 h before use. APTES-treated mica prepared using this specific procedure is called AP-mica.[37]

The graphite surface was cleaved immediately before use.

5.3. Measurements

Static water contact angles were determined with the use of an NRL 100.06 Rami-Hert Inc. (Mountain Lake, NJ) goniometer equipped with a high resolution CCD-IRIS Sony (Sony Corporation, Oradell, NJ) color video camera connected to a computer. Two microliters droplets that were formed at the end of blunt-ended needle of an s1200 Gilmont Instruments (Division of Barnant Co., Barrington, IL) micro-syringe were measured to determine the static contact angles. The measurements were the same within an experimental error of ±1%. Measurements were performed for purified water (Millipore, Billerica, MA), and at an ambient temperature. Three readings of each sample were averaged. Stored images of droplets were analyzed using NIH Image software (National Institutes of Health, Bethesda, MD).

HA was dissolved in water or 0.15 M aqueous sodium chloride to a concentration of 0.5 mg/mL, and rotated overnight to ensure complete dissolution. The solution was further diluted with water to a concentration of 0.1 mg/mL and again rotated overnight; immediately before imaging the solution, the final concentration of 10 μg/mL was prepared by dilution in water. (The difference in final NaCl concentration of 0 M vs 0.003 M did not significantly affect the relative frequencies of observation of different HA conformations.) Samples for imaging were prepared according to the method described by Cowman et al.[10]: 4 μL of the solution were deposited on the substrate, rinsed twice after 2 min with 100 μL of water (unless stated otherwise), and dried under gentle flow of nitrogen. This procedure results in a variable degree of molecular combing of the polysaccharide chains.

Samples were scanned in air with a Digital Instruments Multimode AFM (Veeco Inc., Santa Barbara, CA), equipped with a Nanoscope IIIa controller and an EV scanner, operating in Tapping Mode™. Etched silicon tips TESP7 (Veeco Nanoprobes Inc., Santa Barbara, CA) were used. The roughness of the surfaces was measured using the Multimode 4.43r8 software; the reported value corresponds to the RMS roughness of the whole scanned area.

Acknowledgements

M.K.C. wishes to express her appreciation to David Brant, who has been most helpful as a colleague and mentor, and an inspiration as a scientist.

This work was supported by the Matrix Biology Institute. A. Ulman and A. Korniakov also acknowledge support from the NSF Garcia MRSEC for Polymers at Engineered Interfaces. Portions of this work were presented at the Biophysical Society 2003 annual meeting, San Antonio, Texas, USA, March 2003 and

the Hyaluronan 2003 Conference, Cleveland, Ohio, USA, October 2003.

References

1. Laurent, T. C.; Gergely, J. *J. Biol. Chem.* **1955**, *212*, 325–333.
2. Laurent, T. C.; Ryan, M.; Pietruszkiewicz, A. *Biochim. Biophys. Acta* **1960**, *42*, 476–485.
3. Cleland, R. L. *Biopolymers* **1984**, *23*, 647–666.
4. Fouissac, E.; Milas, M.; Rinaudo, M. *Macromolecules* **1993**, *26*, 6945–6951.
5. Hayashi, K.; Tsutsumi, K.; Nakajima, F.; Norisuye, T.; Teramoto, A. *Macromolecules* **1995**, *28*, 3824–3830.
6. Cowman, M. K.; Matsuoka, S. The Intrinsic Viscosity of Hyaluronan. In *Hyaluronan*; Kennedy, J. F., Phillips, G. O., Williams, P. A., Eds.; Woodhead: Cambridge, 2002; pp 75–78.
7. Mendichi, R.; Šoltés, L.; Giacometti Schieroni, A. *Biomacromolecules* **2003**, *4*, 1805–1810.
8. Cowman, M. K.; Matsuoka, S. *Carbohydr. Res.* **2005**, *340*, doi:10.1016/j.carres.2005.01.022.
9. Gunning, A. P.; Morris, V. J.; Al-Assaf, A.; Phillips, G. O. *Carbohydr. Polym.* **1996**, *30*, 1–8.
10. Cowman, M. K.; Li, M.; Balazs, E. A. *Biophys. J.* **1998**, *75*, 2030–2037.
11. Cowman, M. K.; Liu, J.; Li, M.; Hittner, D. M.; Kim, J. S. Hyaluronan Interactions: Self, Water, Ions. In *The Chemistry, Biology, and Medical Applications of Hyaluronan and its Derivatives*; Laurent, T. C., Ed.; Wenner-Gren International Series No. 72; Portland: London, 1998; pp 17–24.
12. Jacoboni, I.; Valdrè, U.; Mori, G.; Quaglino, D., Jr.; Pasquali-Ronchetti, I. *J. Struct. Biol.* **1999**, *126*, 52–58.
13. McIntire, T. M.; Brant, D. A. Hyaluronic acid self-association in the presence and absence of salts. In *Hyaluronan*; Kennedy, J. F., Phillips, G. O., Williams, P. A., Eds.; Woodhead: Cambridge, 2002; pp 137–140.
14. Al-Assaf, S.; Phillips, G. O.; Gunning, A. P.; Morris, V. J. *Carbohydr. Polym.* **2002**, *47*, 341–345.
15. Cowman, M. K.; Li, M.; Dyal, A.; Balazs, E. A. *Carbohydr. Polym.* **2000**, *41*, 229–235.
16. Cowman, M. K.; Li, M.; Dyal, A.; Kanai, S. Tapping Mode Atomic Force Microscopy of Hyaluronan and Hylan A. In *Hyaluronan*; Kennedy, J. F., Phillips, G. O., Williams, P. A., Eds.; Woodhead Publishing: Cambridge, 2002; pp 109–116.
17. Cowman, M. K.; Spagnoli, C.; Kudasheva, D.; Li, M.; Dyal, A.; Kanai, S.; Balazs, E. A. *Biophys. J.* **2005**, *88*, 590–602.
18. Gribbon, P.; Heng, B. C.; Hardingham, T. E. *Biophys J.* **1999**, *77*, 2210–2216.
19. Gribbon, P.; Heng, B. C.; Hardingham, T. E. *Biochem. J.* **2000**, *350*, 329–335.
20. Kwei, T. K.; Nakazawa, M.; Matsuoka, S.; Cowman, M. K.; Okamoto, Y. *Macromolecules* **2000**, *33*, 235–236.
21. Matsuoka, S.; Cowman, M. K. *Polymer* **2002**, *43*, 3447–3453.
22. Matsuoka, S.; Cowman, M. K. Viscosity of Polymer Solutions Revisited. In *Hyaluronan*; Kennedy, J. F., Phillips, G. O., Williams, P. A., Eds.; Woodhead: Cambridge, 2002; pp 79–88.
23. Cowman, M. K.; Mendichi, R. Methods for Determination of Hyaluronan Molecular Weight. In *Chemistry and Biology of Hyaluronan*; Garg, H. G., Hales, C. A., Eds.; Elsevier Press: Amsterdam, 2004; 41–69.
24. Fujimoto, B. S.; Schurr, J. M. *Biophys. J.* **2002**, *82*, 944–962.
25. Hansma, H. G.; Laney, D. E. *Biophys. J.* **1996**, *70*, 1933–1939.
26. Bustamante, C.; Guthold, M.; Zhu, X.; Yang, G. *J. Biol. Chem.* **1999**, *274*, 16665–16668.
27. Bezanilla, M.; Manne, S.; Laney, D. E.; Lyubchenko, Y. L.; Hansma, H. G. *Langmuir* **1995**, *11*, 655–659.
28. Stokke, B. T.; Elgsaeter, A. *Micron* **1994**, *25*, 469–491.
29. Rivetti, C.; Guthold, M.; Bustamante, C. *J. Mol. Biol.* **1996**, *264*, 919–932.
30. McIntire, T. M.; Brant, D. A. *Biopolymers* **1997**, *42*, 133–146.
31. McIntire, T. M.; Brant, D. A. *J. Am. Chem. Soc.* **1998**, *120*, 6909–6919.
32. Sletmoen, M.; Maurstad, G.; Sikorski, P.; Paulsen, B. S.; Stokke, B. T. *Carbohydr. Res.* **2003**, *338*, 2459–2475.
33. Stokke, B. T.; Brant, D. A. *Biopolymers* **1990**, *30*, 1161–1181.
34. McIntire, T. M.; Penner, R. M.; Brant, D. A. *Macromolecules* **1995**, *28*, 6375–6377.
35. McIntire, T. M.; Brant, D. A. *Int. J. Biol. Macromol.* **1999**, *26*, 303–310.
36. Stokke, B. T.; Falch, B. H.; Dentini, M. *Biopolymers* **2001**, *58*, 535–547.
37. Lyubchenko, Y. L.; Gall, A. A.; Shlyakhtenko, L. S. Atomic Force Microscopy of DNA and Protein–DNA Complexes Using Functionalized Mica Substrates. In *DNA–Protein Interactions: Principles and Protocols*, 2nd ed.; In *Methods in Molecular Biology*; Moss, T., Ed.; Humana: Totowa, NJ, 2001; Vol. 148, pp 569–578.
38. Shlyakhtenko, L. S.; Gall, A. A.; Weimer, J. J.; Hawn, D. D.; Lyubchenko, Y. L. *Biophys. J.* **1999**, *77*, 568–576.
39. Lyubchenko, Y. L.; Shlyakhtenko, L. S. *Proc. Nat. Acad. Sci. U.S.A.* **1997**, *94*, 496–501.
40. Shlyakhtenko, L. S.; Potaman, V. N.; Sinden, R. R.; Lyubchenko, Y. L. *J. Mol. Biol.* **1998**, *280*, 61–72.
41. Herbert, A.; Schade, M.; Lowenhaupt, K.; Alfken, J.; Schwartz, T.; Shlyakhtenko, L. S.; Lyubchenko, Y. L.; Rich, A. *Nucl. Acids Res.* **1998**, *26*, 3486–3493.
42. Oussatcheva, E. A.; Shlyakhtenko, L. S.; Glass, R.; Sinden, R. R.; Lyubchenko, Y. L.; Potaman, V. N. *J. Mol. Biol.* **1999**, *292*, 75–86.
43. Shlyakhtenko, L. S.; Hsieh, P.; Grigoriev, M.; Potaman, V. N.; Sinden, R. R.; Lyubchenko, Y. L. *J. Mol. Biol.* **2000**, *296*, 1169–1173.
44. Shlyakhtenko, L. S.; Miloseska, L.; Potaman, V. N.; Sinden, R. R.; Lyubchenko, Y. L. *Ultramicroscopy* **2003**, *97*, 263–270.
45. Lyubchenko, Y. L. *Cell Biochem. Biophys.* **2004**, *41*, 75–98.
46. Hansma, H. G.; Golan, R.; Hsieh, W.; Lollo, C. P.; Mullen-Ley, P.; Kwoh, D. *Nucl. Acids Res.* **1998**, *26*, 2481–2487.
47. Maurstad, G.; Stokke, B. T. *Biopolymers* **2004**, *74*, 199–213.
48. Martin, A. L.; Davies, M. C.; Rackstraw, B. J.; Roberts, C. J.; Stolnik, S.; Tendler, S. J. B.; Williams, P. M. *FEBS Lett.* **2000**, *480*, 106–112.
49. Lyubchenko, Y. L.; Blankenship, R. E.; Gall, A. A.; Lindsay, S. M.; Thiemann, O.; Simpson, L.; Shlyakhtenko, L. S. *Scanning Microsc.* **1996**(Supp.10), 97–109.
50. Tanigawa, M.; Okada, T. *Anal. Chim. Acta* **1998**, *365*, 19–25.
51. Dunlap, D. D.; Maggi, A.; Soria, M. R.; Monaco, L. *Nucl. Acids Res.* **1997**, *25*, 3095–3101.

52. Fang, Y.; Hoh, J. H.. *Nucl. Acids Res.* **1998**, *26*, 588–593.
53. Allen, M. J.; Bradbury, E. M.; Balhorn, R. *Nucl. Acids Res.* **1997**, *25*, 2221–2226.
54. Spagnoli, C.; Loos, K.; Ulman, A.; Cowman, M. K. *J. Am. Chem. Soc.* **2003**, *125*, 7124–7128.
55. Zhang, Y.; Lu, R.; Liu, Q.; Song, Y.; Jiang, L.; Zhao, Y.; Li, T. J. *Thin Solid Films* **2003**, *437*, 150–154.
56. Lyubchenko, Y. L.; Gall, A. A.; Shlyakhtenko, L. S.; Harrington, R. E.; Jacobs, B. L.; Oden, P. I.; Lindsay, S. M. *J. Biomol. Struct. Dyn.* **1992**, *10*, 589–606.
57. Giesbers, M.; Kleijn, J. M.; Cohen Stuart, M. A. *J. Coll. Interf. Sci.* **2002**, *252*, 138–148.
58. Ray, J.; Manning, G. S. *Langmuir* **1994**, *10*, 2450–2461.
59. Oosawa, F. *Biopolymers* **1968**, *6*, 1633–1647.
60. Ha, B.-Y.; Liu, A. J. *Phys. Rev. Lett.* **1997**, *79*, 1289–1292.
61. Rouzina, I.; Bloomfield, V. A. *J. Phys. Chem.* **1996**, *100*, 9977–9989.
62. Tadmor, R.; Chen, N.; Israelachvili, J. N. *J. Biomed. Mater. Res.* **2002**, *61*, 514–523.
63. Israelachvili, J. N.; Pashlay, R. M. *Nature* **1983**, *306*, 249–250.
64. Hu, J.; Xiao, X.-D.; Ogletree, D. F.; Salmeron, M. *Science* **1995**, *268*, 267–269.
65. Hu, J.; Xiao, X.-D.; Ogletree, D. F.; Salmeron, M. *Surf. Sci.* **1995**, *344*, 221–236.
66. Beaglehole, D. *Physica A* **1997**, *244*, 40–44.
67. Xu, L.; Lio, A.; Hu, J.; Ogletree, D. F.; Salmeron, M. *J. Phys. Chem. B* **1998**, *102*, 540–548.
68. Miranda, P. B.; Xu, L.; Shen, Y. R.; Salmeron, M. *Phys. Rev. Lett.* **1998**, *81*, 5876–5879.
69. Bluhm, H.; Inoue, T.; Salmeron, M. *Surf. Sci.* **2000**, *462*, L599–L602.
70. Cantrell, W.; Ewing, G. E. *J. Phys. Chem. B* **2001**, *105*, 5434–5439.
71. Cheng, L.; Fenter, P.; Nagy, K. L.; Schlegel, M. L.; Sturchio, N. C. *Phys. Rev. Lett.* **2001**, *87*, 156103–156106.
72. Ewing, G. E. *J. Phys. Chem. B* **2004**, *108*, 15953–15960.
73. Chakarov, D. V.; Osterlund, L. O.; Kasemo, B. *Vacuum* **1995**, *46*, 1109–1112.
74. Cabrera Sanfelix, P.; Holloway, S.; Kolasinski, K. W.; Darling, G. R. *Surf. Sci.* **2003**, *532–535*, 166–172.
75. Nagy, G. J. *Electroanal. Chem.* **1996**, *409*, 19–23.
76. Freund, J.; Halbritter, J.; Horber, J. K. H. *Microsc. Res. Tech.* **1999**, *44*, 327–338.
77. Scott, J. E. Secondary Structures in Hyaluronan Solutions: Chemical and Biological Implications. In *The Biology of Hyaluronan*; Ciba Foundation Symposium 143; Wiley: Chichester, 1989; pp 6–20.
78. Winter, H. *J. Phys.: Condens. Matter.* **1996**, *8*, 10149–10183.